JOURNAL OF SOLID STATE CHEMISTRY 3, 145–153 (1971)

The Crystal Structure of the High Temperature Form of Ta_2O_5

N. C. STEPHENSON* AND R. S. ROTH

National Bureau of Standards, Washington, D.C. 20234

Received September 23, 1970

The structure of the high temperature form of Ta_2O_5 can be stabilized by doping with 2 mole% Sc_2O_3 and single crystals have been prepared from a Ta_2O_5–Sc_2O_3 (98:2) composition by the Czochralski technique. The crystal system which at first appeared to be body-centered tetragonal has been determined to be face-centered monoclinic, space group $C2$ with $a = 35.966$ Å, $b = 3.810$ Å, $c = 3.810$ Å, $\beta = 96°7'$. Least-squares refinement cycles reduced the reliability index R to 0.089.

The structure consists of αUO_3-type blocks in which each tantalum atom is surrounded by a pentagonal bipyramid of oxygen atoms. These blocks are infinite in two directions and are separated from similar blocks along a third direction by shear planes. In the vicinity of these shear planes the tantalum atoms are surrounded by distorted octahedral coordination polyhedra.

It is believed that the stabilizing effect of the Sc_2O_3 impurity is due to an increase in the concentration of shear planes. Random shear planes (Wadsley defects) are introduced at approximately 300 Å intervals along the large axis by doping with a substance (Sc_2O_3) which has cations (Sc) large enough to substitute for the host (Ta) but a lower oxygen:metal ratio than the host compound (Ta_2O_5).

Introduction

Ta_2O_5 was first reported to undergo a transformation to a high temperature form by Lagergren and Magneli (*1*). Reisman, Holtzberg, et al. (*2*) reported the phase transition to occur at 1360°C and indicated that the high temperature polymorph probably had triclinic symmetry when quenched to room temperature. Laves and Petter (*3*) and Waring and Roth (*4*) have shown that this form actually undergoes several unquenchable phase transitions upon cooling from high temperatures. For this reason good single crystals of the high temperature form of Ta_2O_5 (H-Ta_2O_5) can not be grown from pure material and examined at room temperature. However, Roth, Waring, and Brower (*5*) have shown that several impurity ions when added to Ta_2O_5 in small amounts enable the apparently tetragonal form of H-Ta_2O_5 to be obtained at room temperature by quenching from above ~1400°C. Furthermore it was demonstrated that large single crystals of this apparently tetragonal H-Ta_2O_5 could be grown by the Czochralski technique utilizing an iridium crucible and about 2–4 mole% Sc_2O_3 as the "stabilizing" impurity ion. A small, annealed, cleavage fragment of one of these crystals has been used in the present study.

As no reasonably good quality crystals of H-Ta_2O_5 have been prepared previously there have not been any prior published attempts to determine the structure. However, Laves, Moser, and Petter (*6*) have pointed out that the structure of H-Ta_2O_5 should probably be similar to that of η (eta) or P-Nb_2O_5. This similarity has been pointed out by Andersson (*7*) and also by Holtzberg (private communication, Sept. 27, 1968). To a first approximation then, H-Ta_2O_5 has been considered to be made up of a series of edge and corner shared octahedra with six molecules in the unit cell instead of the four molecules found in η (P)-Nb_2O_5.

Experimental

Powder photographs of H-Ta_2O_5 stabilized by 2 mole% Sc_2O_3 can be completely indexed on the basis of a tetragonal unit-cell with dimensions $a = 3.810$ and $c = 35.764$ Å. Single-crystal Weissenberg photographs collected with copper radiation, suggested the Laue symmetry $4/mmm$ and small deviations from this symmetry were initially attributed to absorption effects ($\mu = 1146\ cm^{-1}$ for

---

* Permanent address: School of Chemistry, University of New South Wales, Kensington, Australia.

TABLE I

CRYSTAL DIMENSIONS

hkl[a]	*D*[b]	*hkl*[a]	*D*[b]
209	0.010	$10\overline{20}$	0.025
$\bar{2}0\bar{9}$	0.101	010	0.044
$\bar{1}020$	0.025	$0\bar{1}0$	0.044

[a] Indices of each bounding plane.

[b] Perpendicular distance in mm of each plane from an origin at the center of the crystal.

CuKα radiation). Systematic absences in spectra indicated the space group $I4_1/amd$.

For data collection, a single crystal fragment, transparent and roughly tabular in shape (0.02 × 0.05 × 0.09 mm) was mounted about the *b* axis on a single crystal orienter. Intensities were measured by the 2θ scan method with MoK_α radiation. The rate of scanning was 1°/min, and the scan range (SR) was calculated using the equation $\mathrm{SR} = 2.40 + 1.0 \tan\theta$. The backgrounds were measured for 60 sec at $2\theta \pm \frac{1}{2}\mathrm{SR}$. The intensities of three standard reflections were checked periodically during the run to monitor diffractometer and crystal stability. No significant changes were observed in these standards. Data were collected out to 60° in 2θ and one-half of the reciprocal lattice was measured. Counting statistics were used to calculate a standard deviation (σ) for each intensity and if the net number of counts was less than 2σ the reflection was considered as a "less than" and its intensity was set equal to 2σ.

The resulting intensities were corrected for Lorentz, polarization and absorption effects ($\mu = 666\ \mathrm{cm}^{-1}$ for MoK_α radiation). For the latter calculation the crystal measurements listed in Table I were used together with the DATAP program of Coppens, Leiserowitz, and Rabinovich (*8*) to calculate absorption corrections at 125 Gaussian grid points.

The atomic scattering factors for O^{2-} and Ta^{5+} were taken from Suzuki (*9*) and Cromer and Waber (*10*), respectively, and the real part of the anomalous dispersion correction was applied to the scattering curve for tantalum [Dauben and Templeton, (*11*)]. No allowance was made for the scandium content.

Determination of the Structure

The space group $I4_1/amd$ has equivalent positions that are multiples of 4. The twelve tantalum atoms in the unit-cell can therefore be placed in special positions 4*a* or 4*b* and in special positions 8*c*, 8*d* or 8*e*. However, the 30 oxygen atoms (actually 29.76 due to the Sc_2O_3 impurity) cannot be accommodated using the 4-, 8-, 16- and 32-fold equivalent positions unless some positions are fractionally occupied. It seemed probable that the tantalum atoms are indeed distributed in a manner similar to that described above, but the oxygen atoms have a less symmetrical distribution than that required by the space group $I4_1/amd$. In this case, and also because of the short *a* and *b* unit-cell dimensions, a reasonable approach to the structure determination is to initiate a solution in projection using the less extensive plane group symmetries rather than the very large number of space groups that must be considered as alternatives to $I4_1/amd$.

The systematic spectral absences based upon the largest amount of data are those with $h + k + l \neq 2n$. It seemed likely therefore that both (100) and (010) projections would be face-centered. Provided that both of these projections have rectangular symmetry then the plane groups of either projection *must* be *Cm* or *Cmm*.

The (*hol*) Patterson projection is shown in Fig. 1. Tantalum atoms placed in positions 4*a* and 8*e* (with $Z = 0.042$) of space group $I4_1/amd$ provided a satisfactory starting model (Fig. 2a). The plane group corresponding to this atomic arrangement is *Cmm* with atoms in positions 4*e*. Least-squares refinement cycles failed to bring the residual *R* to below 0.30 and symmetry restrictions were therefore relaxed so as to allow the *x* coordinate of the metal atoms to vary. This resulted in an appreciable decrease in *R* (to 0.14) and the correct plane group appeared to be *Cm* with metal atoms in positions 4*b*.

A difference Fourier synthesis clearly showed oxygen atoms in general fourfold positions 4*b* and

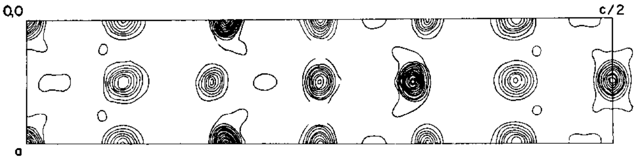

FIG. 1. The hol Patterson function, contoured at arbitrary levels.

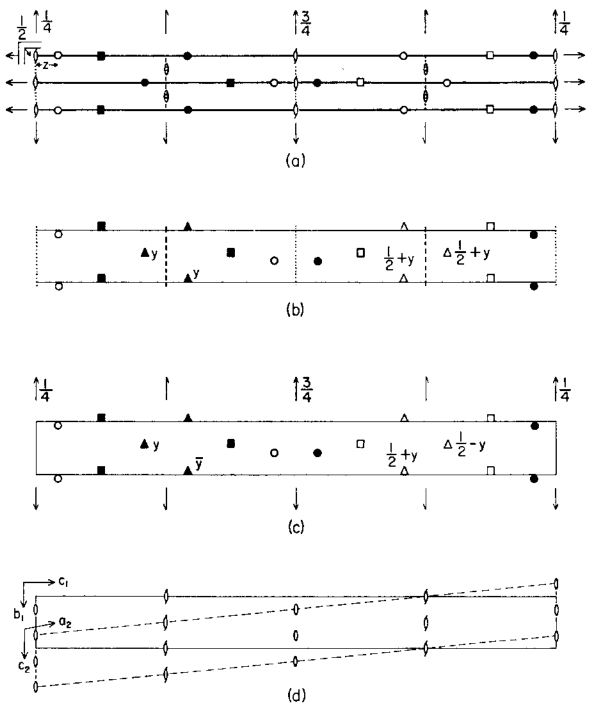

FIG. 2. (a) A trial model in the space group $I4_1/amd$ showing tantalum atoms in positions $4a$ and $8e$ (with $z = 0.042$). Like motifs are related by symmetry elements. Dark motifs represent atoms with $y = \frac{1}{2}$ and clear motifs represent atoms at $y = 0$. The plane group symmetry of the projection is *Cmm*. (b) Some symmetry elements of $I4_1/amd$ can be relaxed to give the space groups *Cc*. The metal atom positions shown in Fig. 2(a) can change slightly but those atoms related across the glide plane at $z = \frac{1}{4}$ have the same y coordinate. The unit-cell shown here is the same as that selected for the tetragonal system and the space group depicted above is therefore *Ic*. (c) The space group *C*2 utilizes some of the symmetry elements of $I4_1/amd$ and these are shown above. Choosing the same orthogonal unit-cell as above, the space group is *I*2 and the atoms either side of the screw axis at $z = \frac{1}{4}$ *do not* have the same y coordinate. (d) The orientation of the correct monoclinic unit-cell of H-Ta_2O_5 with respect to the orthogonal unit-cell chosen on the basis of space group $I4_1/amd$.

Orthogonal cell	Monoclinic cell
$a_1 = 3.810$ Å	$a_2 = 35.966$ Å
$b_2 = 3.810$ Å	$b_2 = 3.810$ Å
$c_1 = 35.764$ Å	$c_2 = 3.810$ Å
Space group $I4_1/amd$	$\beta = 96°7'$
	Space group *C*2

one set in the twofold position $2a$, making a total of 30 in the unit-cell. This correct number of oxygen atoms together with acceptable bond distances and coordination polyhedra, shown in Fig. 3, left no doubt that the model was correct and refinement proceeded smoothly to yield a value of R (*hol*) of 0.086.

The same procedure was tried with the *okl* data. The metal atoms are known to be situated in positions closely related to $4a$ and $8e$ (with $Z \approx 0.042$) of space group $I4_1/amd$ (see Fig. 2a). The (100) projection of this space group also has *Cmm* symmetry but the (001) mirror plane is moved $C/4$ with respect to the position of the equivalent mirror plane in the (100) projection. Attempted refinement of metal atom coordinates in the plane group *Cmm* was not successful but, as before, an acceptably low R value of 0.13 was obtained by allowing both positional parameters of each atom to vary and refining in the plane group *Cm*. Subsequent difference Fourier synthesis, however, failed to show well-formed oxygen peaks either in the correct numbers or which correlated with peaks found for oxygen atoms in the (010) projection.

A reassessment of the situation showed that if the plane groups of the (100) and (010) projections were each *Cm* then the space group for the structure will be *Cc* with the unique axis parallel to c (Fig. 2b). In this case oxygen atoms O(6), shown in projection in Fig. 3 with z coordinates of approximately 0.25,

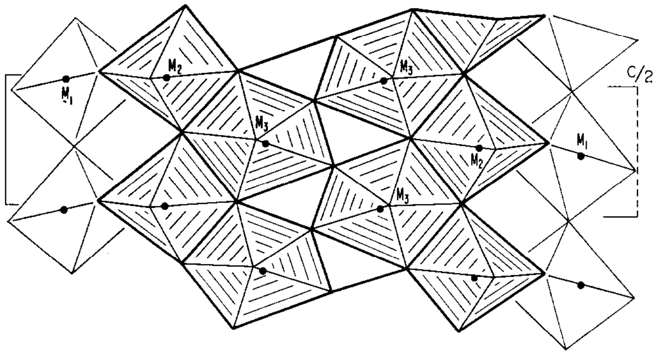

FIG. 3. An (010) projection of the structure of H-Ta_2O_5. Heavily shaded polyhedra are located at $y = \frac{1}{2}$ and the remainder are at $y = 0$.

would have identical coordinates (y) parallel to the projection axis resulting in a close approach between these atoms. The structure of H-Ta_2O_5, as inferred from the (010) projection and known spacial distribution of metal atoms, can be regarded as UO_3-type blocks of Ta–O polyhedra connected to each other by shear planes. In the UO_3 structure [Zachariasen (*12*)], the six oxygen atoms forming the equatorial plane of the hexagonal bipyramidal polyhedra are puckered. A similar arrangement in H-Ta_2O_5 would mean that the oxygen atoms O(6), referred to above, would *not* have the same y coordinates but rather they would be located at y and $\bar{y}$. In this case the glide planes shown in Fig. 2(b) would be replaced by twofold rotation and screw axes, shown in Fig. 2c. The space group becomes $C2$ and the plane group of the projection along the unique axis would be $P2$ rather than Cm, as before.

Refinement of the y and z metal atom coordinates was therefore carried out in the plane group $P2$ and the resulting difference Fourier synthesis clearly showed the correct number of oxygen atoms in positions which correlated with those obtained from the (010) projection. Least-squares refinement cycles reduced R to 0.09.

It was now possible to refine the structural atomic parameters using full three-dimensional data. For correctness the data should be reindexed on the basis of the monoclinic cell whose direct-lattice unit-cell vectors are related to those of the orthogonal cell (defined above) by the transformation matrix.

$$\text{othog (1)} \; \overset{\longrightarrow \text{Mono (2)}}{\boxed{\begin{matrix} 0 & 1 & 0 \\ 0 & 0 & 1 \\ 1 & 0 & 1 \end{matrix}}} \quad \text{(See also Fig. 2d).}$$

This was not done because it was more convenient to refer to the structure in terms of the orthogonal unit-cell that has previously been reported for it [Waring and Roth (*4*)]. The asymmetric quarter of the reciprocal lattice was therefore chosen on the basis of the orientation of the symmetry elements of the space group $I2$ and the programs of Stewart (*13*) were used for the subsequent refinement cycles.

It is doubtful whether a systematic examination of the reciprocal lattice involving a point by point comparison would have revealed the monoclinic symmetry of H-Ta_2O_5. Deviations from tetragonal symmetry are extremely small since the heavy tantalum atoms have essentially a tetragonal distribution. The trial and error method described above makes use of the combined effect of a large number of data and, when used with caution, this approach can be useful in determining the true symmetry, and therefore structure, of a crystal.

The final atomic parameters are listed in Table II and these were used to calculate the final structure factors.[1] The final R value for all observed data is 0.089, and the weighted R value is 0.078.

Description of the Structure

Tantalum atoms $M(3)$ are each surrounded by seven oxygen atoms in the form of a distorted pentagonal bipyramid. Tantalum–oxygen bond distances vary between 1.85(7) and 2.38(4) Å (see Table III) and average at 2.04 Å. The $M(3)$ poly-

---

[1] A table of observed and calculated structure amplitudes from this analysis has been deposited as Document No. NAPS-01227 with the ASIS National Auxiliary Publication Service, c/o CCM Information Corp., 909 3rd Ave., New York, N.Y. 10002. A copy may be secured by citing the document number and by remitting $5.00 for photocopies or $2.00 for microfiche. Advance payment is required. Make checks or money order payable to ASIS–NAPS.

TABLE II

FINAL POSITIONAL AND THERMAL PARAMETERS FOR H-Ta_2O_5[a]

Other atoms in the orthogonal unit-cell are related to those listed below by the symmetry elements of the space group $I2$. Numbers in parenthesis are estimated standard deviations in the least significant digits.

	x/a	y/b	z/c
M(1)	0.00500	−0.00597(80)	0.045682(78)
M(2)	−0.0022(55)	0.49419(82)	0.12514(10)
M(3)	0.4813(29)	0.49882(67)	0.204529(77)
O(1)	0.933(15)	0.501(9)	0.1809(11)
O(2)	0.969(27)	0.488(10)	0.0712(11)
O(3)	0.429(15)	0.492(10)	0.1383(10)
O(4)	0.544(16)	−0.007(10)	0.0526(11)
O(5)	0.458(32)	−0.006(13)	0.1964(14)
O(6)	0.146(19)	0.487(16)	0.2420(14)
O(7)	0.136(24)	0.250	0.0000
O(8)	0.005(46)	0.996(11)	0.1122(12)

	[b]$\beta(11) \times 10^4$	$\beta(22) \times 10^4$	$\beta(33) \times 10^5$	$\beta(12) \times 10^4$	$\beta(13) \times 10^5$	$\beta(23) \times 10^5$
M(1)	189(28)	233(17)	10(2)	53(46)	−56(40)	28(15)
M(2)	318(25)	159(15)	11(2)	−1(44)	−109(40)	33(11)
M(3)	343(33)	28(13)	12(3)	46(42)	−165(40)	30(14)
O(1)	.25(68)[c]					
O(2)	.77(96)					
O(3)	.09(90)					
O(4)	.39(72)					
O(5)	2.17(1.64)					
O(6)	1.42(1.22)					
O(7)	1.01(1.60)					
O(8)	1.39(1.32)					

[a] These parameters are defined with respect to the pseudo tetragonal unit-cell (which has previously been accepted for H-Ta_2O_5).

[b] The form of the anisotropic thermal ellipsoid is

$$\exp\{-[\beta_{11}h^2 + \beta_{22}k^2 + \beta_{33}l^2 + 2\beta_{12}hk + 2\beta_{13}hl + 2\beta_{23}kl]\}$$

[c] The values are $B(\text{Å}^2)$.

hedra share corners with each other and form a sheet two polyhedra wide, which extends infinitely along the a and b directions. The structure within this sheet is very similar to that of UO_3 [Zachariasen, (*12*)].

Tantalum atoms $M(1)$ and $M(2)$ are each surrounded by six oxygen atoms in the form of a distorted octahedron. Each $M(2)$ octahedron shares an edge with an adjacent $M(3)$ pentagonal bipyramid, two edges with $M(1)$ octahedra and is joined with four $M(2)$ octahedra by corner sharing. Each $M(1)$ octahedron shares two edges with $M(2)$ polyhedra and is joined with five other $M(1)$ octahedra by corner sharing. Bond distances for these octahedra are listed in Table III.

Discussion

The crystal structure of H-Ta_2O_5 can thus be viewed as either a modification of the αUO_3 type structure with shear planes to accommodate the difference in cation/anion ratio, or as a combination of αUO_3 blocks with η (P)-Nb_2O_5 blocks. The crystal structure of eta-Nb_2O_5 after Petter and Laves (*14*), is shown in Fig. 4. This structure shows an alternating sequence of four octahedra at zero and one-half for both hOl and Okl projections. The arrangement of octahedra which can be postulated to account for a unit cell with six molecules and a c axis of approximately the length found in H-Ta_2O_5 is shown in Fig. 5. However, this postulated structure

TABLE III

INTERATOMIC DISTANCES (Å) WITHIN EACH COORDINATION POLYHEDRON[a]

M(1) Octahedron		M(2) Octahedron	
M(1)-O(4)^1	1.774(63)	M(2)-O(8)	1.968(42)
O(4)	2.068(63)	O(8)^2	1.952(42)
O(7)	1.967(24)	O(2)^1	1.932(42)
O(8)^2	2.380(42)	O(3)^1	2.217(59)
O(2)^1	2.096(40)	O(1)^1	2.009(39)
O(2)^3	2.138(39)	O(3)	1.709(59)
O(4) -O(7)^1	2.63(7)	O(3) -O(2)^1	2.97(8)
O(7)^1-O(4)^1	3.09(8)	O(2)^1-O(3)^1	3.16(9)
O(4)^1-O(8)^2	2.76(10)	O(3)^1-O(1)^1	2.45(8)
O(8)^2-O(4)	2.96(13)	O(1)^1-O(3)	2.43(8)
O(2)^1-O(7)^1	2.78(5)	O(8) -O(2)^1	2.43(6)
O(4)^1	2.58(9)	O(3)^1	3.06(12)
O(8)^2	2.43(6)	O(1)^1	3.11(6)
O(4)	2.97(10)	O(3)	2.68(10)
O(2)^3-O(7)^1	3.91(9)	O(8)^2-O(2)^1	2.38(8)
O(4)^1	2.62(8)	O(3)^1	3.04(7)
O(8)^2	2.43(6)	O(1)^1	3.13(9)
O(4)	2.99(10)	O(3)	2.66(11)
M(3) Pentagonal Bipyramid			
M(3)-O(5)	1.948(50)		
O(5)^6	1.910(52)		
O(1)	1.917(53)		
O(3)	2.377(39)		
O(1)^1	2.254(57)		
O(6)	1.853(66)		
O(6)^4	2.011(58)		
O(6)^5	2.866(65)		
O(1) -O(3)	2.45(8)		
O(3) -O(1)^1	2.43(8)		
O(1)^1-O(6)	2.33(7)		
O(6) -O(6)^4	2.02(14)		
O(6)^4-O(1)	2.96(10)		
O(5) -O(1)	2.70(10)		
O(3)	2.82(7)		
O(1)^1	2.84(10)		
O(6)	2.76(9)		
O(6)^4	3.04(10)		
O(5)^6-O(1)	2.66(9)		
O(3)	2.82(11)		
O(1)^1	2.80(10)		
O(6)	2.79(8)		
O(6)^4	2.95(10)		

[a] Superscripts refer to symmetry related atoms

No superscript	x,	y,	z,
1	$x-1$,	y,	z,
2	x,	$y-1$,	z,
3	$x-1$,	$y-1$,	z,
4	$\frac{1}{2}+x$,	$\bar{y}$,	$\frac{1}{2}-z$,
5	$x+1$,	y,	z,
6	x,	$y+1$,	z,

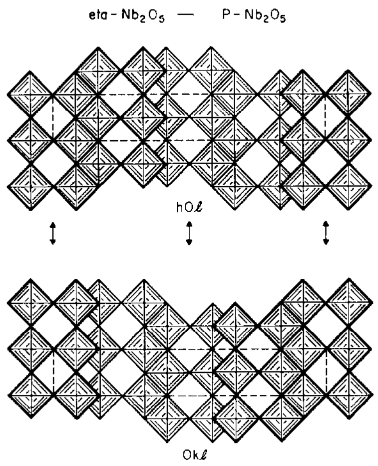

FIG. 4. The crystal structure of $\eta(P)$-Nb_2O_5, after Petter and Laves (*6*).

contains alternating units of six octahedra only in the *hOl* projection; the *Okl* projection shows a sequence of 4-2-4-2. The unit cell is actually face-centered rather than body-centered and the Patterson projections would be quite different for the two projections. Furthermore, the Patterson projection, shown in Fig. 1, for *H*-Ta_2O_5 does not allow an interpretation of six-metal atoms occurring at the same level.

The unit-cell can be forced into a body-centered configuration if the oxygen atom in the twofold site is moved by 1/4 of the 3.8 Å cell edge as shown in Fig. 6. This type of movement has been labelled "1/4 shear" but this nomenclature should not be confused with the term "crystallographic shear" used to describe a change from corner-sharing to

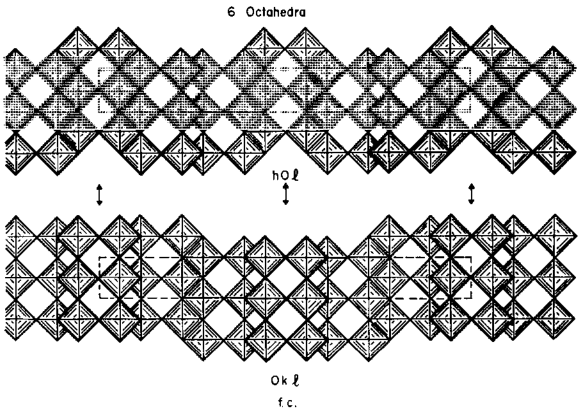

FIG. 5. Hypothetical structure of a phase with six molecules ($B_{12}O_{30}$) with a unit-cell approximately that of *H*-Ta_2O_5, but face-centered.

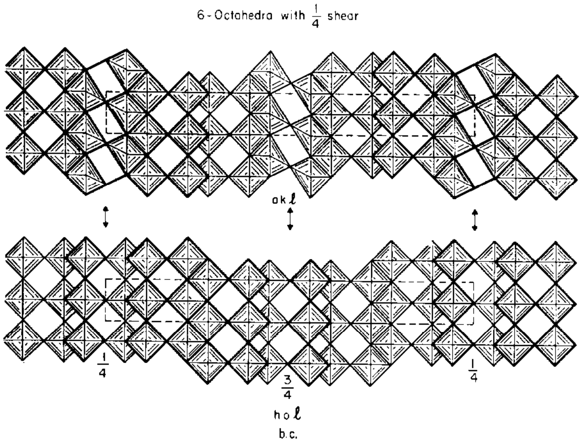

FIG. 6. Hypothetical structure of a phase similar to that of Fig. 5 but with "$\frac{1}{4}$ shear" to form body-centered cell.

edge-sharing of octahedra. Although the new unit-cell shown in Fig. 6 is body-centered the *Okl* projection has six octahedra at each level of the cell while the *hOl* projection has a sequence of 4-1-1-4-1-1. Therefore this structure is still inconsistent with the Patterson projection.

An alternate method to account for the unit cell with six molecules is to intermix units of octahedra and hexagonal bipyramids. Such an arrangement is shown in Fig. 7 with both the octahedra and hexagonal bipyramids drawn as ideal polyhedra for simplicity of construction. This postulated structure consists of a configuration of metal atoms in a 4-1-1-4-1-1 sequence for the *Okl* projection and 4-2-4-2 for the *hOl* projection. However, the unit-cell is face-centered rather than body-centered. The ideal body-centered cell consistent with the Patterson projection of H-Ta_2O_5 can be formulated and is illustrated in Fig. 8 by combining the 1/4-shear feature of Fig. 6 with the mixed octahedra-hexagonal bipyramid scheme of Fig. 7.

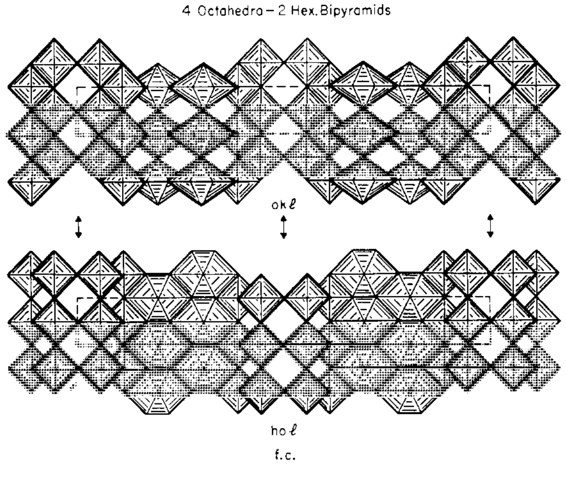

FIG. 7. Hypothetical structure of a phase with approximately the same dimensions as Fig. 5 but containing $\frac{1}{3}$ of the metals in hexagonal bipyramidal coordination.

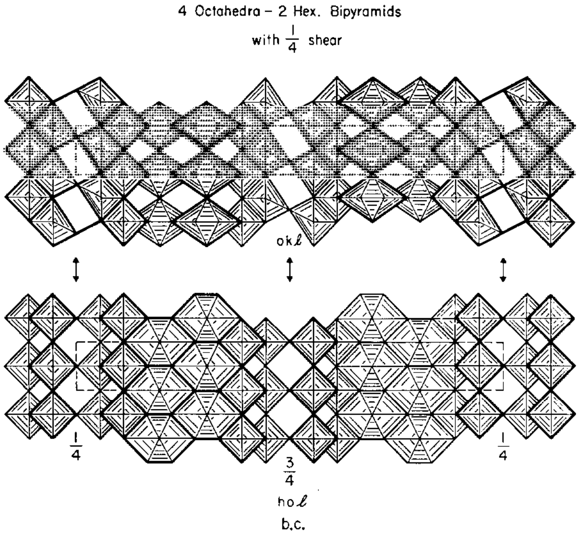

FIG. 8. Ideal structure of H-Ta_2O_5, similar to Fig. 7 but with "$\frac{1}{4}$ shear" to form body-centered cell.

An *Okl* projection of the H-Ta_2O_5 structure, obtained from the two dimensional refinement of the *Okl* data only (Fig. 9) illustrates the fact that the space occupied by the hexagonal bipyramids is actually little greater than that occupied by the octahedra. No attempt has been made in this figure to illustrate that the hexagonal bipyramid is actually distorted into a pentagonal bipyramid as shown in Fig. 3.

In Fig. 10 an infinite array of such hexagonal bipyramids is shown having a total composition of B_2O_6 (B = metal ion) (as in αUO_3). A local reduction in oxygen content can be obtained through

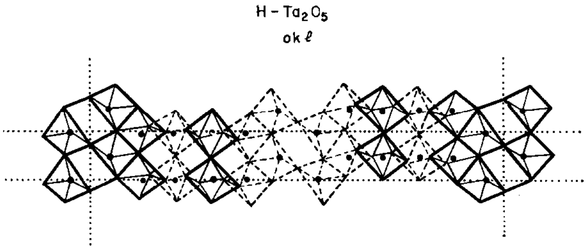

FIG. 9. An *Okl* projection of the H-Ta_2O_5 structure, obtained from the two-dimensional refinement of the *Okl* data only.

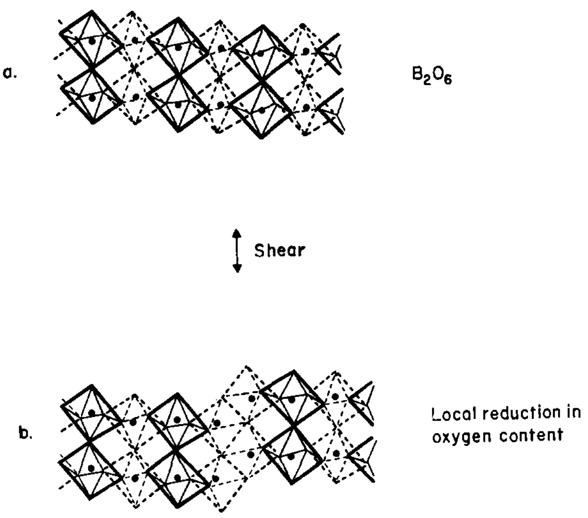

FIG. 10. (*a*) An infinite array of hexagonal bipyramids with a B_2O_6 composition. (b) "Crystallographic shear" results in a local change in coordination to a pair of distorted octahedra and consequent reduction in oxygen content.

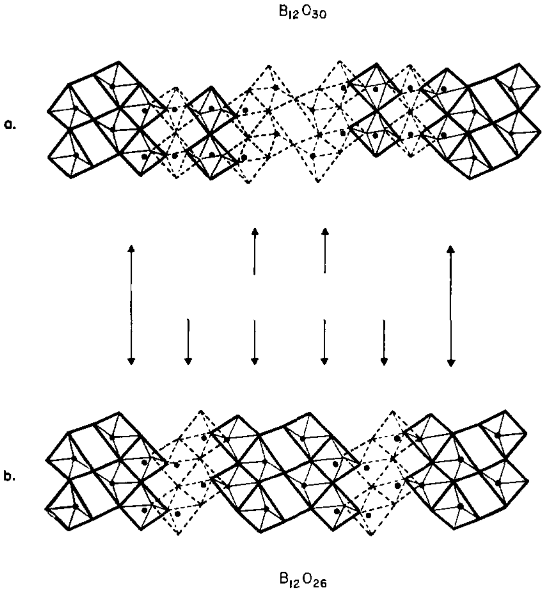

FIG. 11. "Crystallographic-shear" in the *H*-Ta_2O_5 structure. (a) $B_{12}O_{30}$; (b) $B_{12}O_{26}$.

"crystallographic shear" in a plane perpendicular to the figure, as illustrated in Fig. 10b. This crystallographic shear results in two edge-shared octahedra in place of two previously edge-shared hexagonal bipyramids (or corner-shared pentagonal bipyramids). The two metal atoms which were formerly on the same level in the *b* direction and displaced by half the unit cell in *a* are now on the same level in the *a* direction and displaced by half the unit cell in *b*.

Figure 11(a) shows that the phase with the stoichiometry of $B_{12}O_{30}$ (*H*-Ta_2O_5) actually contains four such shear planes per unit-cell and that the octahedra in the structure of *H*-Ta_2O_5 can be considered to be the result of crystallographic shear of an αUO_3 type structure. If such shear is carried to a maximum, the end result [Fig. 11(b)] is a hypothetical phase with a *c* axis of approximately one-half that of *H*-Ta_2O_5 and a stoichiometry of $B_{12}O_{26}$.

It is postulated that the Sc_2O_3 used to stabilize the *H*-Ta_2O_5 crystal structure is accommodated by a replacement of some Ta^{5+} ions by Sc^{3+} and a local reduction in oxygen content by a random shear mechanism similar to that illustrated in Fig. 10(b). Such a random shear has been termed "Wadsley shear" by Andersson (*15*) and this is probably the mechanism which accounts for the solid solutions reported in *H*-Ta_2O_5 [Waring and Roth, (*4*); Roth, Waring, and Brower, (*5*)]. As no superstructure lines have ever been found in *x*-ray patterns of such solid solutions it must be concluded that the shear mechanism is truly random and that these materials are really Wadsley-shear-type nonstoichiometric solid solutions. As each such shear results in a reduction of two oxygen ions per unit-cell a composition of Ta_2O_5:Sc_2O_3 (98:2) would contain about one shear plane every eight unit-cells and the (random) shear planes would be about 286 Å apart.

An attempt to observe these Wadsley defects by the electron microscope lattice image technique (J. Allpress, private communication, 1969) has not been successful due to the *very* excessive damage apparently caused by mechanical shear during grinding of the specimens. A technique such as ion thinning might hopefully prove more fruitful for preparation of specimens for this lattice image examination.

References

1. S. LAGERGREN AND A. MAGNELI, *Acta Chem. Scand.* **6**, 444 (1952).
2. A. REISMAN, F. HOLTZBERG, M. BERKENBLIT, AND M. BERRY, *J. Amer. Chem. Soc.* **78**, 4514 (1956).
3. F. LAVES AND W. PETTER, *Helv. Phys. Acta* **37**, 617 (1964).
4. J. L. WARING AND R. S. ROTH, *J. Res. Nat. Bur. Stand. Sect. A.* **72**, 175 (1968).
5. R. S. ROTH, J. L. WARING, AND W. S. BROWER, JR., *J. Res. Nat. Bur. Stand. Sect. A.* **74**, 485 (1970).

6. F. Laves, R. Moser, and W. Petter, *Naturwissenschaften* **52**, 617 (1965).
7. S. Andersson, *Ark. Kemi.* **26**, 521 (1967).
8. P. Coppens, L. Leiserowitz, and D. Rabinovich, *Acta Crystallogr.* **18**, 1035 (1965).
9. T. Suzuki, *Acta Crystallogr.* **13**, 279 (1960).
10. D. T. Cromer and J. T. Waber, *Acta Crystallogr.* **18**, 104 (1965).
11. C. H. Dauben and D. H. Templeton, *Acta Crystallogr.* **8**, 841 (1955).
12. W. H. Zachariasen, *Acta Crystallogr.* **1**, 265 (1948).
13. J. M. Stewart, Tech. Rep. 67-58, Computer Science Center, University of Maryland, 1967.
14. W. Petter and F. Laves, *Naturwissenschaften* **52**, 617 (1965).
15. S. Andersson, *J. Solid State Chem.* **1**, 306 (1970).